International Journal of Applied Earth Observation and Geoinformation 12 (2010) 9–16

Contents lists available at ScienceDirect

International Journal of Applied Earth Observation and Geoinformation

journal homepage: www.elsevier.com/locate/jag

Determination of land degradation causes in Tongyu County, Northeast China via land cover change detection

Jay Gao [a,*], Yansui Liu [b]

[a] School of Geography, Geology, and Environmental Science, University of Auckland, Auckland, New Zealand
[b] Institute of Geographic Sciences and Natural Resources Research, Chinese Academy of Sciences, Beijing 100101, China

ARTICLE INFO

Article history:
Received 25 February 2009
Accepted 20 August 2009

Keywords:
Land degradation
Rehabilitation of degraded land
Change detection
Landsat TM
Northeast China

ABSTRACT

Tongyu County in Northeast China is highly prone to land degradation due to its fragile physical settings characterized by a flat topography, a semi-arid climate, and a shallow groundwater table. This study aims to determine the causes of land degradation through detecting the long-term trend of land cover changes. Degraded lands were mapped from satellite images recorded in 1992 and 2002. These land cover maps revealed that the area subject to land degradation in the form of soil salinization, waterlogging and desertification increased from 2400 to 4214 km^2, in sharp contrast to most severely degraded land that decreased by 122.5 km^2. Newly degraded land stems from productive farmland (263 km^2), harvested farmland (551 km^2), and grassland (468 km^2). Therefore, the worsened degradation situation is attributed to excessive reclamation of grassland for farming, over cultivation, overgrazing, and deforestation. Mechanical, biological, ecological and engineering means should be adopted to rehabilitate the degraded land.

1. Introduction

As one of the most common and serious environmental problems in the world, land degradation has affected two billion hectares (22.5%) of the world's agricultural land, pasture, forest and woodland (Al Dousari et al., 2000; Oldeman et al., 1990). Severe degradation is blamed for the disappearance of around 5–10 million ha of agricultural land annually. Dryland areas are environmentally fragile, and thus especially susceptible to degradation. It is estimated that global land degradation in drylands causes a loss of land productivity valued around US$13–28 billion a year (Scherr and Yadav, 1996). The livelihood of millions of farmers living in the dryland zone around the world is threatened by degradation of arable farmland. In addition to economic loss associated with reduced land productivity (Bojo, 1991), land degradation also adversely affects the environment. Air and water are polluted by silt, fertilizer and pesticide from farmland. Therefore, it is important to study land degradation and to determine its causes so that it can be reversed.

Land degradation may be studied via several methods, such as field visits and remote sensing. In comparison with the field method, remote sensing method is much more cost-effective and time-efficient in that a huge ground area measured in hundreds of square kilometres can be studied from one image. Remotely sensed imagery is good at revealing the land that has been affected by degradation to various degrees (Gao and Liu, 2008). Remotely sensed data are effective in identifying and mapping land degradation risks (Lu et al., 2007). In particular, remotely sensed satellite data can effectively reveal the spatial extent, magnitude and temporal behaviour of lands affected by waterlogging and subsequent salinization/alkalinization (Sujatha et al., 2000), even though it may be problematic to retrieve remotely sensed primary parameters (such as reflectance) (Hill et al., 1995). Sujatha et al. (2000) mapped the spatial distribution of salt-affected soils, waterlogged areas and eroded lands from visual interpretation of Landsat multispectral scanner and Thematic Mapper (TM) images. A spectral index derived from Advanced Spaceborne Thermal Emission and Reflection Radiometer (ASTER) data has been proposed to characterize the state of land degradation (Chikhaoui et al., 2005). Degraded land can be mapped more than 70% accurately from ASTER data using both per-pixel and object-oriented image classification methods (Gao, 2008a). In addition, MODIS data have been used to estimate local net primary production, from which long-term land degradation in Zimbabwe was detected and mapped (Prince et al., 2009). If combined with GIS, remote sensing can be used to identify areas of land degradation and link them to physiographic settings (Van Lynden and Mantel, 2001). By using remote sensing and GIS, Li et al. (2007)

* Corresponding author. Tel.: +64 9 373 7599x85184; fax: +64 9 373 7434.
E-mail addresses: jg.gao@auckland.ac.nz (J. Gao), liuys@igsnrr.ac.cn (Y. Liu).

0303-2434/$ – see front matter © 2009 Elsevier B.V. All rights reserved.
doi:10.1016/j.jag.2009.08.003

identified land use/cover changes between salinized wasteland and other land covers in the Western part of Northeast China over the last 50 years. The spatial distribution of regional patterns of land degradation can be reliably mapped by using the indices describing the spectrum shape and spectral unmixing (Haboudane et al., 2002). If combined with topographic variables, spectral information is very useful for land degradation assessment.

Monitoring of the long-term trend of land degradation requires consistent and repeatable data that are available for many years. Multitemporal remote sensing data from various sensors spanning over decades are the perfect source for this application. Information on land degradation severity and its process can be efficiently monitored from multitemporal satellite images (Collado et al., 2002). Mapping and monitoring of the evolution of mining-induced land degradation relies on digital analysis of time-series Landsat TM images (Almeida-Filho and Shimabukuro, 2002). Analysis of time-series vegetation index maps derived from Landsat MSS data revealed land degradation in the Northern Province of South Africa (Botha and Fouche, 2000). Chen and Rao (2008) determined the rate and status of grassland degradation in Northeast China from multitemporal Landsat TM/ETM data after the satellite data were converted into land cover maps using the decision tree method.

The determination of the long-term trend of land degradation requires spatial comparison of multiple land cover maps derived from remotely sensed data at different times that must be co-registered with one another to determine spatial changes (Geymen and Baz, 2008). This is commonly known as digital change detection. Change detection can be implemented in several ways, such as change vector analysis (Warner, 2005; Bayarjargal et al., 2006), image differencing (Lu et al., 2005; Desclee et al., 2006), and image rationing (Zhao et al., 2004) of raw spectral bands or results derived from them (e.g., vegetation index). It is also possible to combine these detection methods to identify the process of land degradation. For instance, Adamo and Crews-Meyer (2006) explored desertification processes in West central Argentina based upon analysis of remotely sensed data using vegetation indices, image differentiation, change detection, and pattern metrics. Gomez-Mendoza et al. (2006) projected land use change processes that determine land use change in Sierra Norte of Oaxaca, Mexico. Of all detection methods, post-classification change detection is by far the most popular technique. For instance, Shalaby and Tateishi (2007) monitored land cover and land use changes in the coastal zone of Egypt from Landsat images using the post-classification change detection techniques. This popularity stems from the fact that post-classification change detection is able to reveal not only the nature of change (e.g., from to changes) but also the amount of every possible type of change, even though the detected changes are subject to the accuracy at which each cover is mapped in the respective land cover maps (Gao, 2009).

Whichever change detection techniques are used in the aforementioned studies, they all share one common limitation in that the identified evolution of degraded lands is not linked to specific causes, let alone the proposition of measures for reversing the degradation situation. This study aims to overcome this deficiency by identifying the severity of land degradation through change detection first and then linking the changes in degraded lands to reveal the causes of land degradation. Specifically, the objectives of this study are: (1) to ascertain the severity and spatial distribution of variously degraded lands in Tongyu County, Northeast China through digital analysis of satellite images; (2) to identify the long-term trend of land degradation through tracking of the changes in degraded lands from multitemporal satellite images; and (3) to determine the causes for land degradation through spatial comparison of land cover maps produced. On the basis of the identified causes, appropriate measures will be recommended to rehabilitate the degraded lands for productive uses.

2. Study area

Located in Western Jilin Province, Tongyu County covers a territory of 8459 km^2, extending from 44°13′57″ to 45°16′N in latitude and 122°02′13″ to 123°30′57″E in longitude (Fig. 1). This area has a temperate continental monsoon climate with four distinct seasons. Annual temperature averages 5.1 °C, but extreme temperatures can range from −32 to 38.9 °C. Means annual precipitation amounts to 400–500 mm, 70–80% of which is confined to the summer season, especially July and August when the weather is sunny and hot. By comparison, mean annual evaporation is as high as 1500–1900 mm owing to an abundant supply of solar energy (Li, 2000). Thus, there is a severe water

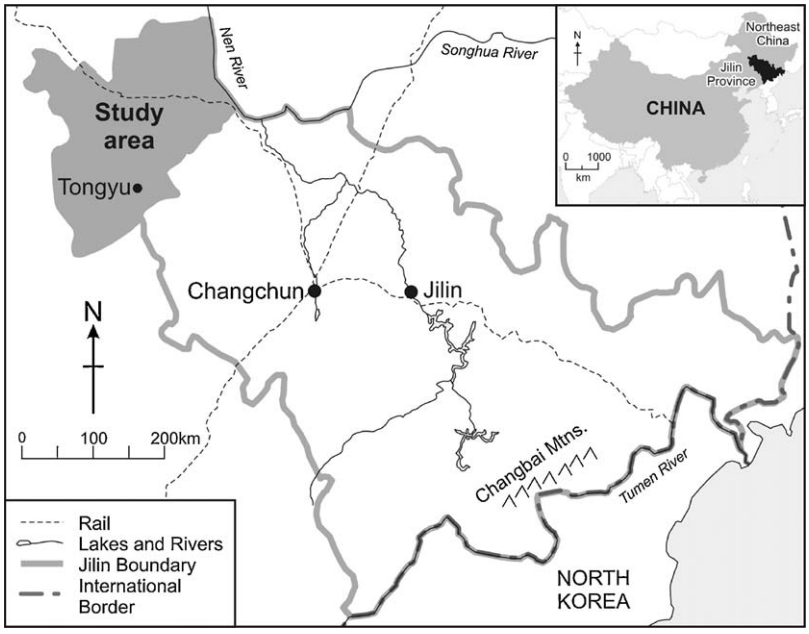

Fig. 1. Location of Tongyu County in relation to China.

deficit. In contrast to water, agricultural land resource is bountiful in Tongyu with per capita arable farmland and grassland being as high as 1.06 and 0.98 ha, respectively. Despite the fragile environment, this land resource has been excessively exploited. Exploitative land use practices such as relentless land reclamation and cultivation have resulted in some land being severely degraded. Land degradation has become a critical factor hindering economic development, achievement of sustainable agriculture, and maintenance of a sound ecosystem in the region.

This area has been selected for study because it exemplifies all the forms of land degradation, including salinization/alkalization, and waterlogging, found in Northeast China. Tongyu is prone to salinization/alkalization owing to an abundant supply of salts and a shallow groundwater table. Weathered granite from tall mountains that flank Tongyu in three directions supplies plentiful soluble salts (chiefly $NaHCO_3$ and Na_2CO_3). They replenish minerals in the groundwater. Consequently, groundwater has a mineral content as high as 0.8 g l^{-1}, much higher than the threshold of 0.5 g l^{-1} for salinization to take place (Li et al., 2002). Moreover, the shallow groundwater is easily elevated to the surface via strong evaporation. Congregation of the soluble salts at or near the land surface alters soil physicochemical properties and leads ultimately to land degradation (Schofield et al., 2001). Tongyu's vulnerability to waterlogging is due to its extremely gentle slope gradient of 1/8000 to 1/500, resulting in little horizontal flow or surface runoff. Thus, rainwater cannot be promptly discharged but accumulates at the surface. Such water cannot percolate down, as the underlying sticky clay is either saturated or impervious. The precipitation regime highly confined to July to August further aggravates waterlogging.

3. Methodology

The satellite data used in this study are two full-scene Landsat TM/Enhanced TM plus (ETM+) images recorded on 18 September 1992 and 22 June 2002, respectively. Both images have been geometrically referenced to the Albers Conical Equal Area projection at a spatial resolution of 30 m. Included in the dataset were six bands. Thermal infrared band six at a spatial resolution different from other bands was excluded. These images were intersected with the boundary of Tongyu County to clip out an identical area. Located inside this area are degraded lands in different forms, including salinization, alkanization, waterlogging and desertification, the first three being the most noticeable.

Prior to image classification, it was decided that land covers inside the study area should be mapped into barren, degraded land, productive (healthy) farmland, fallow (harvested) farmland, grassland, woodland, settled areas, wetland, and water. Although some of these covers are not related to land degradation directly, they are included in the analysis of land cover changes in order to shed light on the anthropogenic causes of land degradation. Barren land refers to denuded land without any vegetative cover as a consequence of waterlogging. Waterlogging exerts a more profound damaging impact on grassland than on farmland that is usually located on a high ground. It represents the most severe form of land degradation. Degraded land refers to salinized and/or alkalized farmland and grassland. Widely spread across the study area, salinization causes reduction in biomass and is responsible for the appearance of whitish image among cropland and grassland on the satellite images. Farmland falls into two categories, healthy, and fallow/harvested. Healthy farmland was full of crops at the time of imaging. Fallow farmland lacked vegetative cover because crops had been harvested or the land had been abandoned for farming. Grassland is the area used for grazing that can be degraded by overgrazing and waterlogging. Woodland refers to any bushes, shrubs, and forest. Settled areas are villages in the middle of fields. Water and wetland are areas covered by water at the time of imaging. Formed from accumulation of rainwater over shallow depressions, water bodies are seasonal lakes lack of any vegetation. Wetland represents shallow water bodies formed from enclosed paleo-channels that have been abandoned for years. Distributed inside wetland are aquatic plants, such as reeds.

This classification scheme was adopted for both sets of Landsat TM images. Training samples were selected for each of the covers in the classification scheme by delimiting polygons around representative sites in ERDAS Imagine®. The pixels enclosed in these polygons were used to derive spectral signature of respective covers on the satellite images. The signature was assessed for spectral separability among all information classes, especially degradation-related covers. Once the spectral signature was deemed satisfactory (e.g., confusion among the land covers to be mapped was minimal), it was input into the classification process in which the satellite data were classified using the supervised maximum likelihood method without prior probability. Two land cover maps of nine types, some of which depicted the type and severity of land degradation, were produced in ERDAS Imagine®. The two maps were later overlaid with each other to identify the spatial changes in degraded land and the trend of land degradation.

4. Results

The severity of land degradation was assessed through areas that were under the influence of degradation in various forms. In 1992 barren land, the most severe form of degradation, covered 464.9 km^2 (25.19%), accounting for 5.5% of the total area (Table 1). In addition, salinization and alkalization affected 1937.2 km^2 of land (22.89%). In total, just over 2400 km^2 of land was subject to land degradation. There were 2131.1 km^2 of harvested farmland, some of which had been abandoned as a consequence of severe salinization. Therefore, nearly half of the County had been influenced by land degradation. Spatially, such degraded land is distributed throughout the study area, but with a higher concentration in the Northeast (Fig. 2). It is heavily juxtaposed with farmland, some of which is bare or harvested while other parts are quite healthy.

At 1760.7 and 2110.7 km^2, respectively, degraded land and harvested/bare farmland became the most prevalent land covers in 2002 apart from healthy farmland (2898.7 km^2, 34.3%) (Table 1). In addition, 342.4 km^2 of land was denuded. This figure would be much higher had harvested/bare farmland been taken into account. Given that the satellite data were recorded on 22 June when vegetation was still growing vigorously, harvested farmland was actually fallow as a result of salinization. It considerably lowers farmland productivity, minimizes the profitability of crop cultivation, and reduces the carrying capacity of grassland. In the worst affected areas, farming has been abandoned altogether. In total, degraded land mounts to 4213.8 km^2, accounting for nearly

Table 1
Mapped land covers and their change from 1992 to 2002.

Cover	1992		2002		Change
	km^2	%	km^2	%	
Farmland-healthy	645.8	7.6	2898.7	34.3	+2252.9
Wetland	296.5	3.5	131.8	1.6	−164.7
Farmland-harvested	2131.1	25.2	1760.7	20.8	−370.4
Woodland	363.8	4.3	214.0	2.5	−149.8
Settlement	231.9	2.7	202.2	2.4	−29.7
Barren land	464.9	5.5	342.4	4.0	−122.5
Degraded	1937.2	22.9	2110.7	25.0	+173.7
Grassland	2107.0	24.9	521.5	6.2	−1585.5
Water	281.4	3.3	277.5	3.3	−3.9
Sum	8459.6	99.9	8459.5	100.1	−0.1

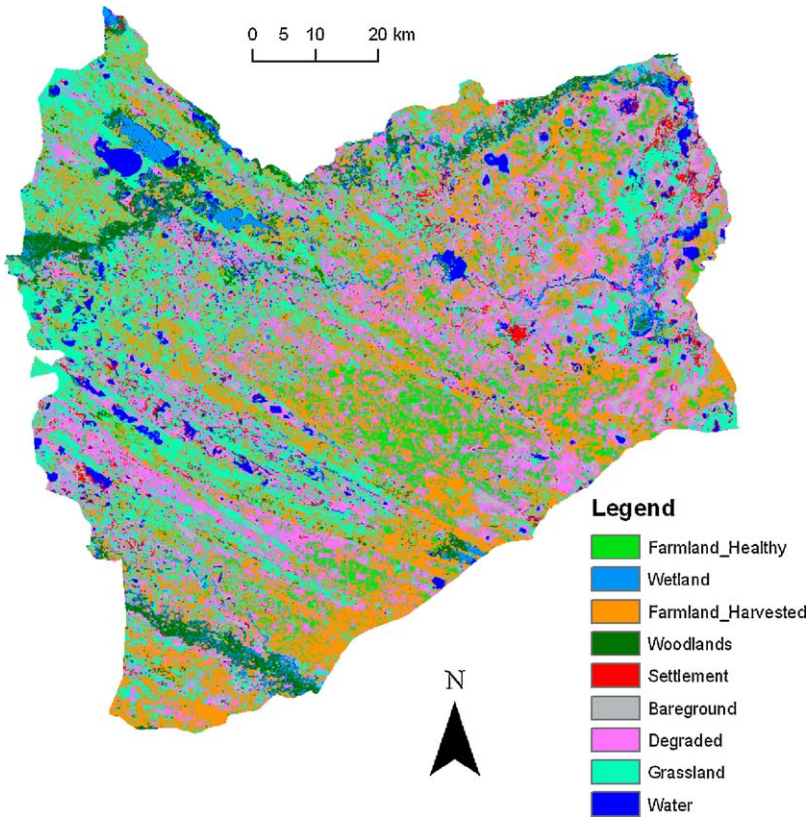

Fig. 2. Distribution of degraded land in 1992, derived from analysis of a Landsat TM image recorded on 18 September 1992.

50% of the area. Most of the degraded land is distributed again in the right half of the study area surrounded by bare/harvested farmland (Fig. 3). This spatial distribution pattern bears a striking resemblance to that shown in Fig. 2.

One of the most noticeable changes in land degradation is the increase in salinized and alkanized land by 173.7 km^2 over the 10-year study period (Table 1). In contrast, barren land was reduced by 122.5 km^2. Similarly, harvested/bare farmland also decreased by 370.4 km^2. This reduction was related partly to the differential timing of imaging (to be analyzed in more detail below). This change pattern suggests that severely degraded areas have decreased while land under the influence of degradation has expanded during the study period. Two other notable changes shown in the table are the huge increase in healthy farmland (2252.9 km^2) and a considerable decrease in grassland (1585.5 km^2). These changes are not pertaining to land degradation directly, but their analysis to be presented in the next section will shed light on the causes of land degradation.

Examination of the conversion among specific land covers (Table 2) is beneficial to ascertain the reasons behind the observed changes. Besides, this spatial comparison is more conducive to revelation of specific changes in the actual area of degraded land than the net figures in Table 1. Representing the break down of their counterparts in Table 1, figures in Table 2 illustrate all the possible changes between any two covers. Some of these figures having a low value are probably not genuine as a result of misclassifications. However, they do not affect the general trend of land degradation. In order to reveal this trend, this section concentrates on the critical changes. For instance, 262.9 km^2 of healthy farmland and 551.4 km^2 of harvested farmland became degraded during 1992–2002. These changes indicate that over cultivation of crops in this vulnerable environment has contributed to land degradation. Furthermore, 468.0 km^2 of grassland was also degraded during the study period. Similar to farmland, grassland is vulnerable to degradation if its carrying capacity is exceeded. The decrease in woodland by 149.8 km^2 is due to conversion to farmland (e.g., land reclamation through deforestation), urbanization, and flooding. These changes are indicative of a deteriorating degradation situation that may worsen in the future.

At a first glance, the increase in healthy farmland from 645.8 km^2 in 1992 to 2898.7 km^2 has nothing to do with land degradation. Nevertheless, it is still worthwhile to explore the reasons for this rise. The first cause for the increase is related to the changed timing of the images from 18 September to 22 June when most crops were still growing vigorously. The second, more worrying cause of this increase is the loss of grassland at 1585.5 km^2. As shown in Table 2, 1143.9 km^2 of grassland was converted into healthy farmland. Thus, the newly gained farmland was created through reclamation of grassland in the eastern half of the County. Although this land was identified as healthy at the time of study (June 2002), it is questionable whether this will be the case in the future. Given the vulnerable environmental settings in the study area, newly reclaimed farmland is highly susceptible to degradation. Possibly, this part of the study area may follow the suit of its counterpart in the right half.

5. Discussion

5.1. Use of the satellite data

In change detection studies, the multitemporal remote sensing data used should ideally be anniversary in order to avoid any potential artificial changes related to phonology in vegetation-related covers. In this study the TM/ETM+ data were recorded at a span from June to September. While this temporal discrepancy may cause some artificial changes to the detected results, it will

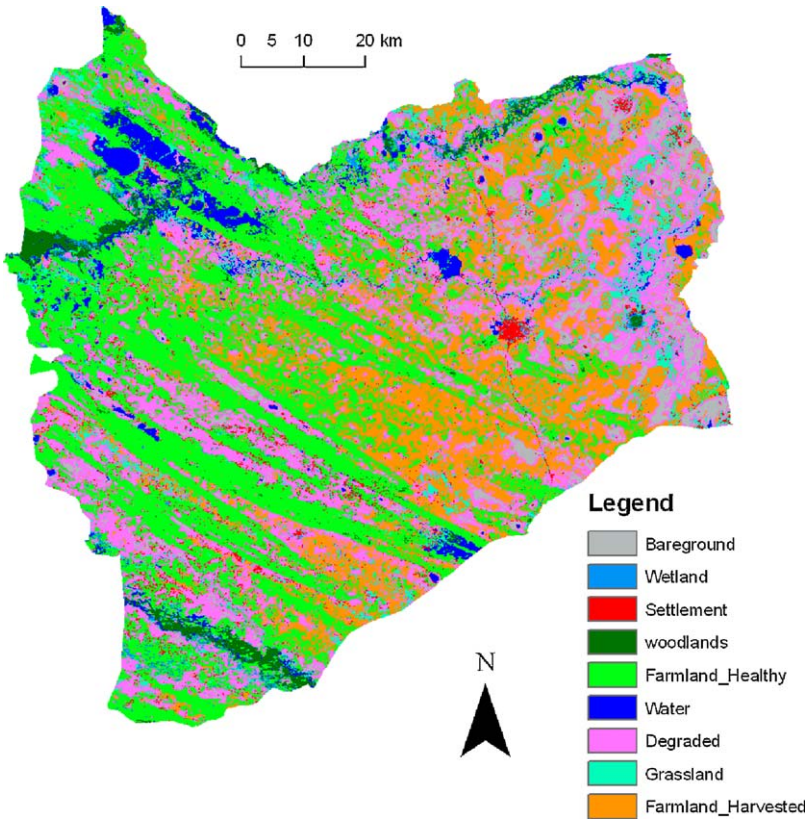

Fig. 3. Distribution of degraded land in 2002, derived from analysis of a Landsat TM image recorded on 22 June 2002.

Table 2
Change in land covers between 1992 and 2002 (unit: km^2)[a].

Land cover	1	2	3	4	5	6	7	8	9	Sum
1. Farmland-healthy	98.7	447.4	0.6	34.8	7.7	4.9	0.5	0.2	50.9	645.8
2. Farmland-harvested	1256.2	522.2	1.5	**111.2**	33.0	16.9	0.8	2.0	187.3	2131.1
3. Woodland	66.3	1.1	156.0	17.5	3.4	41.7	63.1	0.6	14.1	363.8
4. Grassland	**1143.9**	208.7	1.2	153.8	54.0	23.4	1.8	52.3	**468.0**	2107.0
5. Settled	10.2	10.5	1.9	13.4	17.0	4.3	2.8	45.9	125.9	231.9
6. Wetland	21.9	3.2	48.8	33.0	7.2	18.7	106.1	4.3	53.3	296.5
7. Water	14.4	5.2	3.1	26.3	18.4	5.4	99.9	28.4	80.3	281.4
8. Barren land	24.3	10.9	0.1	7.9	7.9	0.8	0.8	127.1	**285.0**	464.9
9. Degraded	262.9	**551.4**	0.8	123.7	53.7	15.8	1.5	81.6	845.8	1937.2
Sum	2898.7	1760.7	214.0	521.5	202.2	131.8	277.5	342.4	2110.7	8459.5

Boldfaced figures: indicative of degradation causes.
[a] Across: land cover in 1992; down: land cover in 2002.

not fundamentally alter the change between degraded and non-degraded land. In this sub-arctic region June lies at the beginning of the growing season while September approaches the end of the growing season. Such timing minimizes the discrepancy between non-degraded and degraded land. Although there may be some artificial changes between healthy and harvested farmland due to the timing, they will not contaminate the amount of land that has been degraded. Therefore, the temporal discrepancy is not an issue of concern.

In this study no accuracy assessment was carried out for either of the land cover maps in Figs. 2 and 3 because the primary focus of this study is the causes of land degradation. Presented in Table 3 is an accuracy assessment for a Landsat TM image of 1989 of the study site. Although the mapped area was much smaller in that study, the accuracy should be replicable to the entire County as the same mapping method was applied to the same type of data. According to this error matrix, degraded land was mapped at an accuracy level of 75%, but slightly more accurate for barren land (80%). There is some confusion between barren and degraded, and between degraded and grassland. The former confusion takes place between two types of land degradation, and is thus not a concern. The later confusion may change the area of degraded land. Nevertheless, it is anticipated that the confusion would be very similar in both land cover maps in Figs. 2 and 3. Thus, some confusion was cancelled out during change detection via image subtraction. Even if residual confusion still persisted in the change detection results, it should not be large enough to invalidate the general trend of land degradation detected in the study area.

5.2. Causes of land degradation

A large amount of healthy farmland and harvested farmland were degraded during the study period. Degradation of such lands stems from the mutual interaction between the vulnerable natural settings and anthropogenic factors. Natural settings conducive to land degradation include a flat topography dotted with enclosed

Table 3
Error matrix of the results classified from a 1989 TM image. Across: classified; down: reference ($\kappa = 0.7739$)[a].

Cover	1	2	3	4	5	6	7	8	9	Sum	User's accuracy (%)
1. Barren	20		3							25	80%
2. Settled	2	7	3		2			8	3	25	28
3. Degraded	1		30		2		5	2		40	75
4. Wetland			1	24						25	96.0
5. Grassland					28			1	6	35	80.0
6. Woodland				1		19				20	95
7. Water							25			25	100.0
8. Fallow		1			2			27		30	90
9. Farmland					1			5	24	30	80.0
Sum	23	8	37	25	35	19	30	43	33	255	
Producer's accuracy (%)	87.0	87.5	81.1	96	80	100	83.3	62.8	72.7		80.0

[a] *Source*: Gao (2008b).

channels, and a semi-arid climate, in addition to an abundant supply of soluble salts and a shallow groundwater table. The landscape is dotted with many abandoned paleo-channels that are enclosed or partially enclosed. Soil in the vicinity of these water bodies suffers from severe salinization. In this temperate continental monsoon region, rainfall coincides with hot weather, creating an excellent opportunity for evaporation to take place. At 1200–1400 mm per annum, it is nearly three times annual precipitation. Evaporation carries soluble salts in the soil and groundwater to the Earth's surface. In the dry season water in some shallow depressions is completely evaporated, leaving severely salinized land behind.

The human economic activities that are primarily responsible for initiating land salinization and exacerbating the degradation situation can be summed up as irrational and abusive land use practices, such as massive land reclamation for grain cultivation, overgrazing and deforestation. In order to produce more grain to feed the ever growing population, over half (1143.9 km^2) of the grassland in 1992 were reclaimed for farming. Accompanying this reclamation was removal of surficial vegetation, which accelerated evaporation and transport of mineral salts from deep down to near the surface in this salinization-prone environment. The reduced vegetative coverage, in return, sped up surface moisture evaporation during which salts were transported from deep down to near the surface. Accumulation of these salts creates an unfavourable environment for plants to survive. Ploughing also brings former salt-rich soil to the surface. Land reclamation has turned the former degradation potential into a reality. Over cultivation is the direct cause of land degradation.

Degradation of 468.0 km^2 of grassland in this agro-pastoral intertwining region is caused by overgrazing. In the late-1980s animal husbandry expanded explosively in sharp contrast to grassland productivity that remained unchanged or even reduced as a result of land degradation. For instance, grassland productivity averaged 1350 kg ha^{-1} over West Jilin in 1985. The existing grassland resources could support 5.4 million goats or their equivalent (e.g., consumption of the same quantity of forage), slightly lower than the actual stock size of 5.86 million goats or their equivalent (Bai, 2000). By the end of 2000, the average grassland productivity decreased to only 600 kg ha^{-1}. Theoretically, the amount of forage yield could support 2.30 million goats or their equivalent, against the actual stock size of 12.06 million. With such a large breeding size, the grassland was consumed and tramped nearly constantly with little chance for recovery. Over a long period of time, grassland degradation becomes irreversible and the land degrades to barren.

Over the study period woodland decreased its acreage from 363.8 to 214 km^2 or by a net decrease of 149.8 km^2. Deforestation is thus another anthropogenic factor responsible for the worsening degradation situation. After the market economy was introduced in the late-1970s, 66.3 km^2 of woodland was cleared for short-term economic gain and/or for farming, together with shrubland and natural forest. The shrinkage of natural elm forest and shrubland on a massive scale drastically damaged the effectiveness of protection afforded by forest and windbreaks. It is much easier for soil to lose its moisture in the semi-arid region. Without such protection, newly created farmland was easily damaged, resulting in increased soil erosion, the internal cause of potential land desertification (Li et al., 2004).

5.3. Rehabilitation of degraded lands

Rehabilitative measures fall into two categories: passive and active. Passive measures refer to those actions that can halt adverse impacts on the environment without heavy investment, such as termination of the abusive land use practices conducive to land degradation. The improperly reclaimed farmland from grassland should be returned to grazing to minimize its vulnerability to degradation. Since grassland degradation is caused primarily by overgrazing, rehabilitation of degraded grassland can be achieved by reducing grazing intensity to a sustainable level. The number of herds that can be supported by the grassland resource should be based strictly on grassland carrying capacity. Those severely overgrazed areas should be sealed off from grazing to give the grass a chance to regenerate. For instance, grazing should be banned temporarily during April to June each year when the grass just turns green (Li et al., 2002). One strategy to achieve this is to partition the grassland into different zones and each zone is grazed in turn. Another strategy is to breed the stock in captivity. These passive methods emphasizing natural recovery are very effective at rehabilitating slightly and moderately degraded areas where land degradation is still reversible.

Rehabilitation of irreversibly degraded lands requires active measures that aim at reducing soil salinity/alkalinity and restoring the capability of degraded land through heavy human intervention and investment, even though these measures may not bring any tangible benefits immediately. There are four of them: mechanical, biological, ecological, and engineering (Jiang et al., 2006). Mechanical measures rehabilitate degraded land through altering soil physical and chemical properties via external materials. Degraded soil becomes sticky when wet but strong when dry. It has a compact structure with little porosity. These properties can be improved via application of organic fertilizer, animal manure, organic waste, and crop remains on top of salinized soil (Li et al., 2003). Rich in humus, these organic matters are able to improve soil structure, fertility and reduce its salinity. The improved soil structure, in turn, can then provide a better condition for plants to thrive. The alkalinity of the top soil can also be neutralized by chemicals such as gypsum, zeolite, and aldonic residue (Sheng et al., 2002). The use of aldonic residue is particularly effective in

improving soil properties. Its high humus content is highly effective in neutralizing soil alkalinity and changing its pH value.

Biological means aim at reducing soil salinity and reversing the deteriorating degradation situation through establishing a healthy vegetative cover. This is usually achieved by planting salt-tolerant crops such as sunflowers, beetroot and barley. In addition to their economic return, these crops are also able to absorb soil salts without any negative effects (Li et al., 2002). Once these crops become established, soil salts can be expected to decrease in future cycles. The reduced soil salinity creates a favourable environment for other cash crops to grow and thrive. Biological means may be combined with mechanical means to alter the physical and chemical properties of soil.

Ecological means emphasizes the restoration of the degraded ecosystem so that the degradation situation can be halted. Land degradation can be minimized by plantation of trees and salt-tolerant plants (Li and Zhen, 1995). Through planting trees of salt-tolerant species, the windbreak system may be conserved and protected. The improved ecosystem can help reverse the spiral effect of continuous degradation. In those waterlogging-prone areas, salt-tolerant plants (e.g., *Suaeda glauca*, *Atriplex patens Iljin*, *Polygonaceae* and reeds) may be planted after the land has been treated with the mechanical remedy measures described above. Although these plants only bring minimal economic returns (e.g., reeds may be used to make pulp), they are good at absorbing soil salts and hence reducing soil salinity. Besides, vegetative protection can prevent the contamination of adjacent land by salts blown away from bare ground.

Engineering means takes the form of construction of water conservancy facilities. Irrigation canals can prevent the accumulation of rainwater on the surface during the rainy season, and hence avoid concentration of salts over shallow depressions. Water saved by the conservancy facilities can be used to irrigate crops in the dry season. The saved water can also be used to flood the salinized land to dissolve salts. Irrigation also helps to partly remove soil salts and reduce soil salinity through dilution.

Of the four measures, the mechanical method requires a lot of labour input. It is best applied to rehabilitating degraded farmland. The biological and ecological measures do not require huge investment. Once the protective system is established, it can bring lasting benefits over a long period. The engineering method requires a huge amount of monetary investment. It might be true that the benefits generated from the rehabilitation efforts may not be adequate to compensate for the investment over a short-term. However, even severely salinized land can become productive economically and ecologically through a proper combination of the four rehabilitative measures.

6. Conclusions

Digital analysis of two Landsat images recorded at an interval of 10 years showed that the area under the influence of soil salinization/alkanization, waterlogging and desertification increased from 2400 to 4214 km^2 in Tongyu County in Western Jilin Province of Northeast China. Newly degraded land originates from productive farmland (263 km^2), harvested farmland (551 km^2), and grassland (468 km^2). The total area of land under the influence of degradation increased from less than 25% in 1992 to 50% in 2002, reaching 4213.8 km^2. On the other hand, severely degraded land decreased from 464.9 to 342.2 km^2. Therefore, land degradation is still expanding while the most severely degraded land has been brought under control. During the study period healthy farmland increased by 2252.9 km^2, in sharp contrast to grassland that decreased by 1585.5 km^2. The causes of land degradation are thus identified as excessive reclamation of grassland as farmland, over cultivation, overgrazing and deforestation. Such exploitive land use practices have resulted in an increase in the saline-alkali area and exasperated the severity of land degradation, causing former slightly degraded land to become moderately degraded. These anthropogenic factors, in conjunction with the vulnerable environmental settings, such as an extremely gentle topography at a gradient of 1/5000 to 1/8000, a shallow groundwater table, strong evaporation exceeding precipitation, and an abundant supply of minerals, have turned the potential of land degradation in the study area into a reality.

It is proposed that grazing and farming be reduced or halted to lessen the degradation situation. The degraded land may be rehabilitated to productive use via a combination of mechanical, biological, ecological and engineering measures. The integrated application of these measures should help to halt the worsening of the degraded ecosystem in this fragile environment.

Acknowledgments

This research received financial support from the National Natural Science Foundation of China (grant numbers 40871257 and 40635029). We are grateful to Ms. Ling Chun Tung who provided some assistance in data analysis. Two anonymous reviewers provided helpful comments in improving the quality of the manuscript.

References

Adamo, S.B., Crews-Meyer, K.A., 2006. Aridity and desertification: exploring environmental hazards in Jachal, Argentina. Applied Geography 26 (1), 61–85.
Al Dousari, A.M., Misak, R., Shahid, S., 2000. Soil compaction and sealing in AL-Salmi area, Western Kuwait. Land Degradation and Development 11, 401–418.
Almeida-Filho, R., Shimabukuro, Y.E., 2002. Digital processing of a Landsat TM time series for mapping and monitoring degraded areas caused by independent gold miners, Roraima State, Brazilian Amazon. Remote Sensing of Environment 79, 42–50.
Bai, X., 2000. A Study on the Ecological Environment and the Establishment of an Ecological Province in Jilin. Jilin University Press, Changchun (in Chinese).
Bayarjargal, Y., Karnieli, A., Bayasgalan, M., Khudulmur, S., Gandush, C., Tucker, C.J., 2006. A comparative study of NOAA-AVHRR derived drought indices using change vector analysis. Remote Sensing of Environment 105 (1), 9–22.
Bojo, J.P., 1991. Economics and land degradation. Ambio 20, 75–79.
Botha, J.H., Fouche, P.S., 2000. An assessment of land degradation in the Northern Province from satellite remote sensing and community perception. South African Geographical Journal 82 (2), 70–79.
Chen, S., Rao, P., 2008. Land degradation monitoring using multi-temporal Landsat TM/ETM data in a transition zone between grassland and cropland of Northeast China. International Journal of Remote Sensing 29 (7), 2055–2073.
Chikhaoui, M., Bonn, F., Bokoye, A.I., Merzouk, A., 2005. A spectral index for land degradation mapping using ASTER data: application to a semi-arid Mediterranean catchment. International Journal of Applied Earth Observation and Geoinformation 7 (2), 140–153.
Collado, A.D., Chuvieco, E., Camarasa, A., 2002. Satellite remote sensing analysis to monitor desertification processes in the crop-rangeland boundary of Argentina. Journal of Arid Environments 52, 121–133.
Desclee, B., Bogaert, P., Defourny, P., 2006. Forest change detection by statistical object-based method. Remote Sensing of Environment 102 (1–2), 1–11.
Gao, J., 2008a. Mapping of land degradation from ASTER data: a comparison of object-based and pixel-based methods. GIS Science and Remote Sensing 45 (2), 149–166.
Gao, J., 2008b. Detection of changes in land degradation in Northeast China from Landsat TM and ASTER data. In: Proceedings of the XXIth Congress of ISPRS. Beijing, China, 3–12 July (CD-ROM).
Gao, J., 2009. Digital Analysis of Remotely Sensed Imagery: Chapter 13—Multitemporal Image Analysis. McGraw-Hills, New York, 645 p.
Gao, J., Liu, Y., 2008. Mapping of land degradation from space: A comparative study of Landsat ETM+ and ASTER data. International Journal of Remote Sensing 29 (14), 4029–4043.
Geymen, A., Baz, I., 2008. The potential of remote sensing for monitoring land cover changes and effects on physical geography in the area of Kayisdagi mountain and its surroundings (Istanbul). Environmental Monitoring and Assessment 140 (1–3), 33–42.
Gomez-Mendoza, L., Vega-Pena, E., Ramirez, M.I., Palacio-Prieto, J.L., Galicia, L., 2006. Projecting land-use change processes in the Sierra Norte of Oaxaca, Mexico. Applied Geography 26 (3–4), 276–290.
Haboudane, D., Bonn, F., Royer, A., Sommer, S., Mehl, W., 2002. Land degradation and erosion risk mapping by fusion of spectrally-based information and digital geomorphometric attributes. International Journal of Remote Sensing 23, 3795–3820.

Hill, J., Sommer, S., Mehl, W., Megier, J., 1995. Use of Earth observation satellite data for land degradation mapping and monitoring in Mediterranean ecosystems: towards a satellite-observatory. Environmental Monitoring and Assessment 37 (1–3), 143–158.

Jiang, D., Zong, W., Li, X., Liu, Z., Yan, Q., He, S., 2006. Rehabilitation of desertified lands in Western Horqin steppe. Chinese Journal of Ecology 25 (3), 243–248 (in Chinese).

Li, F., He, Y.F., Liu, Z.M., Zhang, B., 2004. Dynamics of sandy desertification and its driving forces in Western Jilin Province. Chinese Geographical Science 14, 57–62.

Li, J., Zhen, H., 1995. Ecological restoration of the alkali-saline land in the Songnen Plain and the optimal model of restoration. Journal of Northeast Normal University (Natural Science Edition) 27 (3), 67–71.

Li, Q.S., Li, X.J., Li, X.S., Wang, Z.C., Song, C.C., Zhang, G.X., 2003. Sodium bicarbonate soil management and utilization in Songnen Plain. Resources Science 25 (1), 15–20 (in Chinese).

Li, X.J., 2000. The alkali-saline land and agricultural sustainable development of the Western Songnen plain in China. Scientia Geographica Sinica 20, 51–55 (in Chinese).

Li, X.J., Li, Q.S., Wang, Z.C., Liu, X.T., 2002. A research on characteristics and rational exploitation of soda saline land in the Western Songnen Plain. Research of Agricultural Modernization 23, 361–364 (in Chinese).

Li, X.J., Wang, Z., Song, K., Zhang, B., Liu, D., Guo, Z., 2007. Assessment for salinized wasteland expansion and land use change using GIS and remote sensing in the West part of Northeast China. Environmental Monitoring and Assessment 131 (1–3), 421–437.

Lu, D., Batistella, M., Mausel, P., Moran, E., 2007. Mapping and monitoring land degradation risks in the Western Brazilian Amazon using multitemporal Landsat TM/ETM+ images. Land Degradation and Development 18, 41–54.

Lu, D., Mausel, P., Batistella, M., Moran, E., 2005. Land-cover binary change detection methods for use in the moist tropical region of the Amazon: a comparative study. International Journal of Remote Sensing 26 (1), 101–114.

Oldeman, R.L., Hakkeling, R.T.A., Sombroek, W.G., 1990. World Map of the Status of Human-induced Soil Degradation: An Explanatory Note. International Soil Reference and Information Centre, Wageningen, Netherlands.

Prince, S.D., Becker-Reshef, I., Rishmawi, K., 2009. Detection and mapping of long-term land degradation using local net production scaling: application to Zimbabwe. Remote Sensing of Environment 113, 1046–1057.

Scherr, S.J., Yadav, S., 1996. Land Degradation in the Developing World: Implications for Food, Agriculture, and the Environment to 2020. Food, Agriculture, and the Environment Discussion Paper 14, International Food Policy Research Institute, Washington, DC, 35 p.

Schofield, R., Thomas, D.S.G., Kirkby, M.J., 2001. Causal processes of soil salinization in Tunisia, Spain and Hungary. Land Degradation and Development 12, 163–181.

Shalaby, A., Tateishi, R., 2007. Remote sensing and GIS for mapping and monitoring land cover and land-use changes in the Northwestern coastal zone of Egypt. Applied Geography 27 (1), 28–41.

Sheng, L.X., Ma, X.F., Wang, Z.P., 2002. Study on the recovery and control of the alkali-saline lands in Songnen Plain. Journal of Northeast Normal University 34 (1), 30–35.

Sujatha, G., Dwivedi, R.S., Sreenivas, K., Venkataratnam, L., 2000. Mapping and monitoring of degraded lands in part of Jaunpur district of Uttar Pradesh using temporal spaceborne multispectral data. International Journal of Remote Sensing 21, 519–531.

Van Lynden, G.W.J., Mantel, S., 2001. The role of GIS and remote sensing in land degradation assessment and conservation mapping: some user experiences and expectations. International Journal of Applied Earth Observation and Geoinformation 2001 (1), 61–68.

Warner, T., 2005. Hyperspherical direction cosine change vector analysis. International Journal of Remote Sensing 26 (6), 1201–1215.

Zhao, G.X., Lin, G., Warner, T., 2004. Using Thematic Mapper data for change detection and sustainable use of cultivated land: a case study in the Yellow River delta, China. International Journal of Remote Sensing 25 (13), 2509–2522.